03,13

The effect of temperature on the electron-stimulated desorption of lithium atoms from the surface of Li_xAu_y intermetallic compounds

© Yu.A. Kuznetsov, M.N. Lapushkin

Ioffe Institute,
St. Petersburg, Russia

E-mail: lapushkin@ms.ioffe.ru

Received April 18, 2023
Revised April 18, 2023
Accepted April 20, 2023

The effect of temperature on the electron-stimulated desorption of lithium atoms from the surface of 2D semiconductor Li_xAu_y intermetallic compounds in the temperature range from 160 to 300 K was studied. Li_xAu_y intermetallic compounds were formed during the deposition of lithium atoms on gold film 2 monolayers thick at room temperature. An island mechanism for the formation of Li_xAu_y intermetallic compounds has been proposed. The decrease in the yield of electronically stimulated desorption of lithium atoms from the surface of Li_xAu_y 2D semiconductor intermetallic compounds with decreasing temperature is associated with a decrease in the probability of capturing an excited electron into the conduction band into a local state near the bottom of the conduction band. The calculation by the density functional method showed that 2D layers of LiAu form semiconductor compounds, the band width of which decreases with increasing thickness of the 2D layers of LiAu.

Keywords: electron-stimulated desorption, lithium, gold, semiconductor, intermetallic compound.

DOI: 10.61011/PSS.2023.07.56409.64

1. Introduction

Intermetallic compounds are defined as compounds of two and more metals, properties of intermetallics can differ from the properties of their components. This is the reason why intermetallics are widely used in various areas: from space industry and medicine to jewelry. The simplest intermetallics consist of two metals among which alkali-metal-gold compounds can be distinguished. The key feature of these intermetallics include the fact that gold serves as the anion, rather than the cation like in most of gold compounds [1]. This is due to the fact that gold has the highest electronegativity ($\chi = 5.77$ eV) among all metals which is close to the electronegativity of halogens (for At $\chi = 5.87$ and for I $\chi = 6.76$ eV). However, the gold atom can transfer its electron only to atoms with low electronegativity [1], e.g. alkali metal atoms (for Cs $\chi = 2.18$ eV). The study of CsAu [2] launched the investigations of alkali-metal-gold intermetallics. Bimetallic compounds can produce compounds semiconductors: non-metallic nature of alkali-metal-gold intermetallics was shown for the first time in the first half of the 20th century in [3]. This study showed that CsAu is a wide-band semiconductor with a band gap of 2.8 eV. Investigations of RbAu intermetallic [4] and KAu and NaAu calculations [5] have shown that they are metals. It should be noted that CsAu is an ionic semiconductor and charge transfer from the alkali metal to gold decreases in Cs-Li row [6]. Experimental results are confirmed by the electronic structure calculations of these materials, for example [6–10].

Few studies have investigated lithium atom adsorption on gold. In [7], photoemission investigations of Li−Au interaction on Ru(001) surface were carried out and showed that a thin Au film with a thickness of 5 monolayers acquires a metal nature after adsorption of Li atoms on it. In [8], it was shown that intermetallic Li_xAu_y 2D semiconductors were formed when Li atoms were deposited on a thin gold film on tungsten by the electron-stimulated desorption (ESD) method at 300 K.

Transition from 3D materials to 2D materials delivered an unexpected result: 2D alkali-metal-gold intermetallic films were found to be able to form compound semiconductors and actually form compound semiconductors. Formation of 2D Na_xAu_y [9] and K_xAu_y intermetallics [10] when sodium and potassium atoms are deposited on gold at $T = 1000$ K results in formation of compound semiconductors. It should be noted that 2D Na_xAu_y layer is a wide-band semiconductor with a band gap of 2.7 eV [9]. Formation of 2D alkali-metal-gold films was confirmed for Li_xAu_y [8], Na_xAu_y [11], K_xAu_y [12] and Cs_xAu_y [13] intermetallics by the electron-stimulated desorption (ESD) method. ESD of neutral atoms with excitation energy lower than 200 eV is observed only on semiconductor and dielectric surfaces [14,15]. ESD is not observed from metallic surfaces at these excitation energies due to fast relaxation of excited electron states [14,15]. Relaxation time of excited electron states in a semiconductor (dielectric) is sufficient for execution of various Auger processes resulting in ESD of atoms [14,15].

Formation of alkali-metal-gold intermetallics during deposition of alkali metal atoms on a gold substrate at

temperatures close to room temperature and below is a two-stage process. At the first stage which corresponds to deposition of alkali-metal-gold pre-monolayer coatings, intermetallic is not formed. Only after deposition of the alkali metal monolayer coating, the second stage starts and is associated with alkali metal atom diffusion into a gold substrate with formation of intermetallic compounds. It should be noted that the gold monolayer nearest to the surface is not involved in the intermetallic formation process when alkali metal atoms are deposited on the 2D gold film applied to the tungsten surface [16].

The objective of this study was to investigate temperature dependences between the electron-stimulated desorption of lithium atoms deposited on the gold film and formation of Li_xAu_y semiconductor intermetallics and to calculate the density of 2D LiAu layers having different thicknesses by the density functional method to determine at which 2D layer thicknesses LiAu is a semiconductor and becomes a metal.

2. Experiment

2.1. Materials

Tungsten ribbons were used as substrates for the test samples. The ribbons were pre-heated at 1800 K in oxygen at $1 \cdot 10^{-6}$ Torr during 3 h. Gold was deposited on the ribbon at 300 K from a directly heated tungsten tube where 99.99% purity gold foil pieces were placed, and lithium was deposited on the ribbon at 300 K from a directly heated evaporator by thermal reduction of lithium oxide with aluminum. Concentration of lithium atoms on the ribbon surface was determined by the time of constant-flux deposition, whose intensity was measured by surface ionization current on the Ir ribbon and was equal to $1.0 \cdot 10^{15}$ atom/cm^2 in the Li atom monolayer (MLs). Concentration of the deposited Au was determined by the time of constant-Au flux deposition, which was calibrated by means of thermal desorption spectroscopy, and was equal to $1 \cdot 10^{15}$ atom/cm^2 in the Au atom monolayer. The experiments were carried out in the temperature range from 160 to 300 K.

2.2. Preparation of samples

The following sample preparation method was used: a pre-defined amount of gold was deposited on a clean tungsten ribbon at room temperature and then a variable amount of lithium atoms was deposited as appropriate for the ESD measurements. After the measurements, the tungsten surface was cleaned and prepared again. It should be noted that the Au atom monolayer on the tungsten surface is not involved in formation of Li_xAu_y compound in this method.

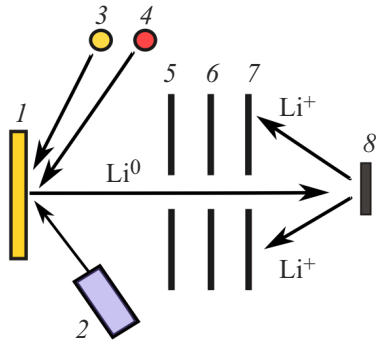

Figure 1. Experiment diagram. *1* — sample, *2* — electron source, *3* and *4* — Au and Li evaporators, *5, 6* — electrodes that retain ions being desorbed when the sample is irradiated by electrons, *7* — ion collector, *8* — surface ionization ribbon.

2.3. Experimental setup

The investigations described herein were carried out in „Spectrometer ESD“ super-high-vacuum unit whose experimental diagram is shown in Figure 1. Residual gas pressure in the unit was below $5 \cdot 10^{-10}$ Torr. The experiments were carried out at T from 160 to 300 K. The tungsten ribbon with Li_xAu_y layer deposited on it was exposed to 0–200 eV electron beam. Power delivered by the electron beam did not changed the ribbon temperature. Li atoms being desorbed were ionized on the iridium ribbon heated up to 2000 K. At this temperature, surface ionization probability of Li atoms is equal to one [17]. ESD of atoms is characterized by the ESD yield (q) which is equal to the desorbed atom flux density vs. the ESD-exciting electron flux density. „Spectrometer ESD“ unit recorded the ESD yield of Li atoms, measured the dependence of this yield q on the energy of the exciting electrons, measured the distribution by kinetic energies of desorbed atoms and the amount of Li and gold deposited on the substrate.

2.4. Calculation details

Calculations were carried out in QUANTUM ESPRESSO package [18] using the exchange-correlation functional taking into account the Perdew-Burke-Ernzerhof (PBE) [20] generalized gradient approximations (CGA) [19]. The influence of ion cores was considered through a norm-conserving pseudopotential [21]. Supercells (111) $2 \times 2 \times 2$ were prepared using BURAI-1.3 open source GUI software [22]. Kinetic energy limit and charge density limit were set to 55 Ry and 550 Ry. Gamma-centered grid by k-points $4 \times 4 \times 1$ was used for all 2D layers in this study. Convergence was equal to $1 \cdot 10^{-6}$ Ry. Geometry optimization was carried out by relaxation of all atom positions in the supercell, except the outer gold atom layer until a pressure lower than 0.5 kbar and force applied to each atom lower than 0.01 eV/Å are achieved. Vacuum gap was set to 18 Å to avoid collapse of 2D layers relative to each other and to ensure geometrical relaxation.

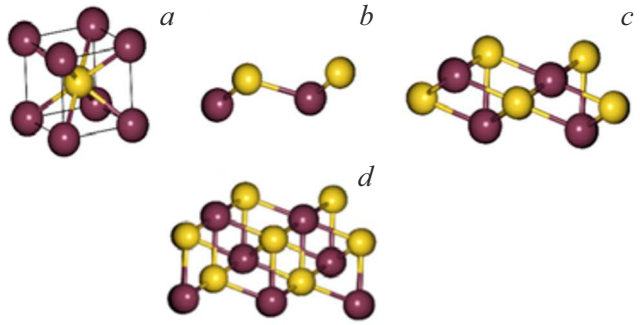

Figure 2. LiAu (a) crystal structure. 2D LiAu layers: one LiAu monolayer (b), two LiAu monolayers (c), three LiAu monolayers (d). Yellow ball — gold atom, dark-red ball — lithium atom.

LiAu has a CsCl structure with a lattice constant of 3.11 Å [6] (Figure 2, a). Supercells contain one to three LiAu layers. 2D layers LiAu layer structure is shown in Figure 2.

3. Results and discussion

3.1. Electron-stimulated desorption

It is known that no intermetallics are formed when alkali metal atoms are deposited on the monolayer gold film on tungsten (see diagram a in Figure 3).

Figure 4 shows the Li atom ESD yield vs. Li atom deposition dose on 2D gold film consisting of two monolayers on the tungsten substrate for two substrate temperatures (160 and 300 K). It can be seen that when the Li atom deposition dose is lower than one monolayer, Li atom ESD is not observed. This is due to the fact that submonolayer Li atom coating is formed on the surface and Li atom diffusion into the 2D gold film does not occur and the film is still metallic (see Diagram b in Figure 3). When deposition dose (DD_{Li}) is more than one monolayer, ESD of Li atoms occurs which indicates that a gold-lithium intermetallic compound semiconductor is formed under the subsurface Li atom monolayer. Reported ESD of Li atoms shows that the formed intermetallic is a semiconductor. The first measured point corresponds to $DD_{\mathrm{Li}} = 1.1$ MLs from which only the number of Li atoms corresponding to 0.1 MLs of Li can react with intermetallic formation. Taking into account that the gold monolayer nearest to the tungsten surface is not involved in intermetallic formation, then it would be reasonable to assume that $LiAu_{10}$ intermetallic will form.

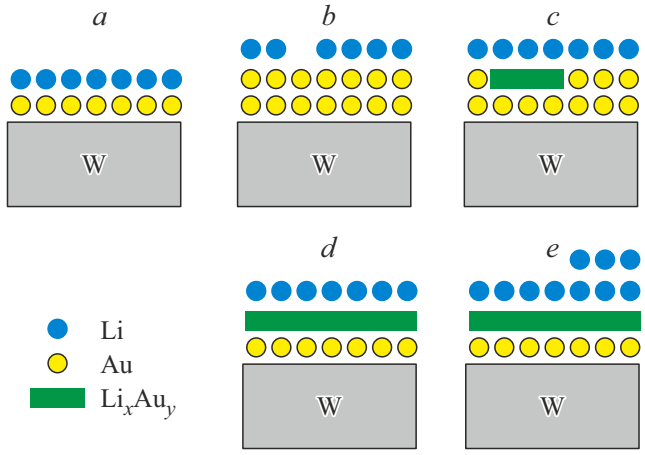

Figure 3. Diagram of Li and Au deposition on W: for 1 Au monolayer and 1 Li monolayer(a), for 2 Au monolayers and Li submonolayer coverage (b), for 2 Au monolayers and deposition dose of 1.5 Li monolayer with formation of 2D Li_xAu_y layer (c), for 2 Au monolayers and deposition dose of 2.0 Li monolayer with formation of 2D LiAu layer (d), for 2 Au monolayers and deposition dose of 2.5 Li monolayer with formation of 2D LiAu layer (e).

Intermetallic with such stoichiometry obviously will be metallic. This suggests that Li_xAu_y semiconductor islands with stoichiometry close to LiAu are formed (see diagram c in Figure 3). Further increase in Li atom deposition dose results in higher Li atom ESD yield which is indicative of area growth by Li_xAu_y semiconductor islands. Maximum Li atom ESD yield is achieved at $DD_{\mathrm{Li}} = 2.0$ MLs. Whilst LiAu intermetallic formation is expected (see Diagram d in Figure 3). Further increase in Li atom deposition dose results in lower Li atom ESD yield which is associated with the fact that no Li atom diffusion into the gold-lithium intermetallic occurs at $DD_{\mathrm{Li}} > 2.0$ MLs, but the second Li atom monolayer is formed preventing the Li atom yield (see Diagram e in Figure 3). This indicates that the ESD process takes place at the intermetallic – adsorbed lithium interface. It can be seen that the ESD yield at 300 K is 1.6 times higher than at $T = 160$ K.

Figure 5 shows Li atom ESD yield from the tungsten surface coated with two gold monolayers at the deposition dose of two Li monolayers at $T = 300$ (1) and 160 K (2) vs. the bombarding electron energy of (E_e). Two wide peaks are observed at the excitation energy of 63.5 and 81.4 eV. These peaks are associated with the excitation of Au $5p_{3/2}$ and Au $5p_{1/2}$ core levels with bond energy (E_b) 57.2 and 74.2 eV, respectively. Relation of areas under peaks is equal to 0.71 which is close to spin-orbit relation equal to 0.67. Peak width at half maximum (Γ) for 300 K is equal to 8.8 and 9.4 eV, respectively, for peaks with maxima at 63.5 and 81.4 eV. When temperature decreases to 160 K, Γ increases for the peak with bond energy 63.7 up to 9.6 eV, and remains unchanged for the peak with bond energy 81.3 eV. It should be noted that the peak with excitation energy 81.4 eV is symmetric for all studied temperatures and it shape does not change with temperature. However, the peak with maximum at 63.5 eV is asymmetric, drawn towards high excitation energies and its shape changes with lower temperature and higher peak width. This can suggest that an additional Li atom ESD channel exists. We assume that excitation of Li 1s level core peak with bond energy $E_b = 54.7$ eV probably occurs resulting in peak broadening and asymmetry. The existing

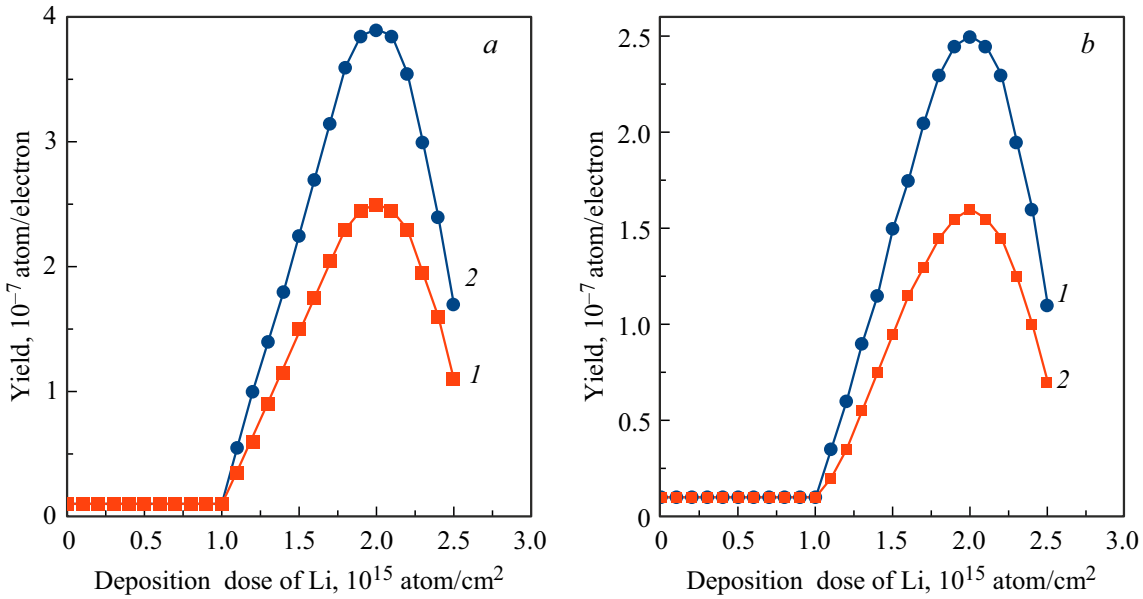

Figure 4. *a*) Li atoms yield q in ESD from tungsten coated with two gold monolayers with $T = 160$ (*1*) and 300 K (*2*) vs. Li atom deposition dose DD_{Li} for a bombarding electron energy of 64 eV. *b*) Li atom yield q in ESD from the tungsten surface coated with two gold monolayers at $T = 160$ K for an excitation energy of 64 (*1*) and 82 eV (*2*) from Li atom deposition dose.

data is not sufficient to support this assumption therefore additional investigations are required.

Figure 4, *b* shows Li atom yield during ESD from the tungsten surface coated with two gold monolayers at $T = 160$ for an excitation energy of 64 eV and 82 eV from Li atom deposition dose. Behavior of Li atom ESD yield for both excitation energies vs. Li atom deposition dose curves is similar.

Figure 6 shows dependences of the Li atom ESD yield with two gold monolayers and deposition dose of $DD_{\mathrm{Li}} = 2.0$ MLs at which maximum ESD yield is achieved

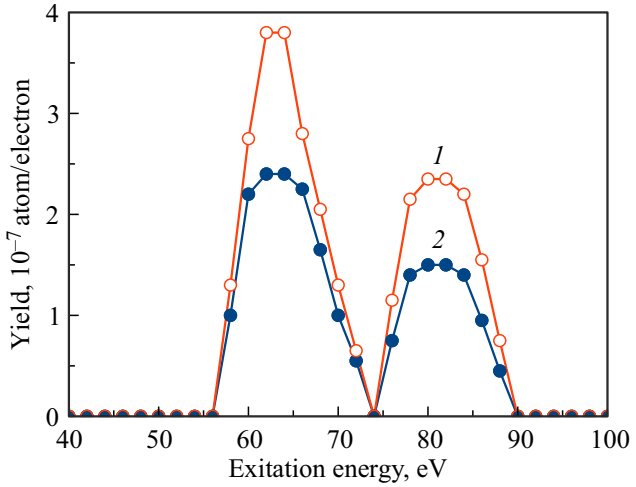

Figure 5. Li atom yield q during ESD from the tungsten surface coated with two gold monolayers at the deposition dose of two Li monolayers at $T = 300$ (*1*) and 160 K (*2*) vs. the bombarding electron energy of E_e.

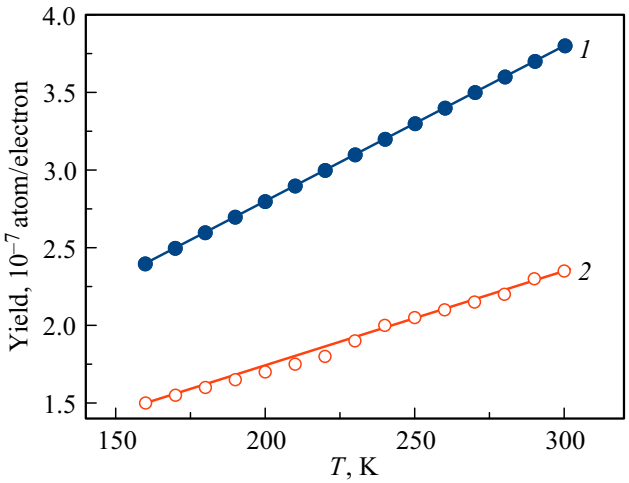

Figure 6. Li atoms yield q during ESD from tungsten coated with two gold monolayers at Li atom deposition dose $DD_{\mathrm{Li}} = 2$ MLs depending on the substrate temperature for bombarding electron energy of 64 (*1*) and 82 eV (*2*).

for exciting electron energy 64 eV and 82 eV from the substrate temperature in the range from 160 to 300 K. It can be seen that Li atom ESD yield dependences grow almost linearly with temperature growth. However, a faster growth takes place for the yield with 64 eV electron excitation than for 82 eV electrons. The corresponding slopes of lines $q(E_e)$ differ by a factor of 4. This may be due to the fact that the probability of ESD process associated with Li 1s level excitation with bond energy $E_b = 54.7$ eV grows faster with temperature than the probability of ESD process

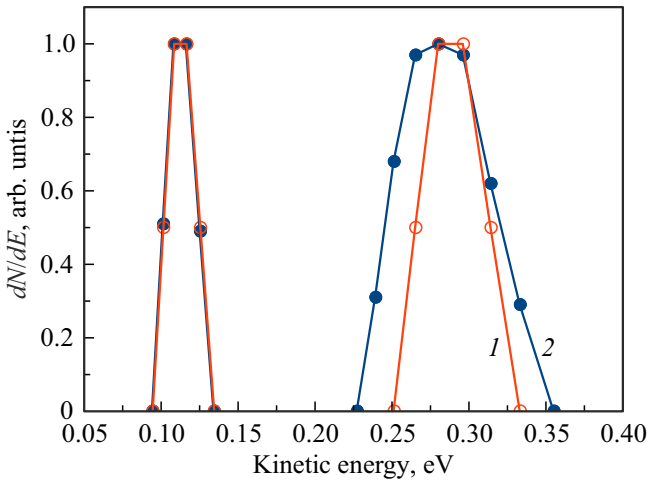

Figure 7. Normalized distributions by kinetic energies E_{kin} of Li atoms during ESD from the W surface coated with two Au monolayers at Li atom deposition dose $DD_{Li} = 2$ MLs at 300 K, for bombarding electron energy 64 eV for deposition dose MLs for two temperatures 160 (*1*) and 300 K (*2*).

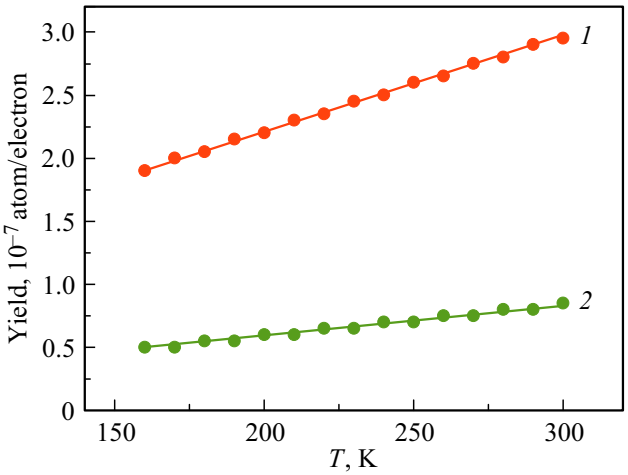

Figure 8. Temperature dependence of Li atom yield during ESD from the W surface coated with two Au monolayers at Li atom deposition dose $DD_{Li} = 2$ MLs at 300 K for bombarding electron energy 64 eV for: for high-energy peak (*1*) and low-energy peak (*2*).

associated with Au $5p_{3/2}$ level excitation with bond energy $E_b = 57.2$ eV. This can also be affected by the fact that the Li atom ESD process may involve not only atoms included in the intermetallic, but also those included in the surface Li atom monolayer. It should be noted that the rate of Li atom diffusion from the intermetallic through the surface Li atom monolayer also grows with temperature.

Figure 7 shows temperature influence on the normalized distributions by kinetic energies E_{kin} of Li atoms during ESD from the W surface coated with two Au monolayers at 300 K, for bombarding electron energy 64 eV for deposition dose MLs for two temperatures 160 and 300 K. The spectrum at $T = 300$ K has two peaks: low-energy (LE) at 0.11 eV and high-energy (HE) at ~ 0.27 eV. Similar to the previous studies [8,11,12], it would be reasonable to assume that the LE peak is associated with excitation of lithium atom desorption from the intermetallic layer, and the HE peak is associated with excitation of lithium atom desorption from the Li atom monolayer nearest to the intermetallic surface. The narrow LE peak position does not depend on temperature, while the HE peak is shifted towards high energies by 0.01 eV and becomes more narrow with its Γ decreasing from 0.067 to 0.042 eV.

Figure 8 shows temperature dependences of Li atom yield during SD from the W surface coated with two Au monolayers at Li atom deposition dose $DD_{Li} = 2$ MLs at 300 K for bombarding electron energy 64 eV for: for high-energy peak and low-energy peak. It can be seen that linear growth of Li atom ESD yield takes place. However, the HE peak growth occurs faster than the LE peak: the curve slope for the HE peak is three times as high as for the LE peak. This indicates that desorption from the surface Li atom monolayer becomes more preferable with temperature growth than the Li atom desorption from the LiAu intermetallic (because we assume that it is intermetallic with stoichiometry 1 : 1 that is formed at the deposition dose of 2 Li atom monolayers on the gold film 2 monolayers in thickness.

The diagram of electronic transitions during Li atom ESD from the gold-lithium intermetallic surface was earlier published in [8] for sample temperature 300 K. Consider the main processes occurring during the Li atom ESD and temperature influence on the processes. Electron irradiation of the surface results in the excitation of Au $5p_{3/2}$ and Au $5p_{1/2}$ core levels with formation of a hole on them and electron transition to a local state near the conduction band bottom. Further, the hole is neutralized due to various Auger transitions. The electron near the conduction band bottom goes to the conduction band and then is captured on vacant states of Li atoms. Li atom become neutral, larger and is pushed out from the surface, i.e. desorbed. The observed temperature dependences of the Li atom ESD yield may be explained by the fact that the probability of transition from the local state to the conduction band is reduced with lower temperature.

3.2. Electronic structure

The calculation uses a simplified model consisting of isolated 2D LiAu layers, because the alkali metal monolayer–2D intermetallic layer–gold monolayer–tungsten substrate system is rather complicated for calculations. Using a simplified model, the change in the electronic structure of the intermetallic with growth of 2D layer thickness can be assessed qualitatively.

The calculation results for LiAu crystal cell and 2D LiAu layers with different thickness are shown in Figure 9.

Calculations results for density of states (DOS) of LiAu crystal are shown in Figure 9, *d*. As expected, it follows

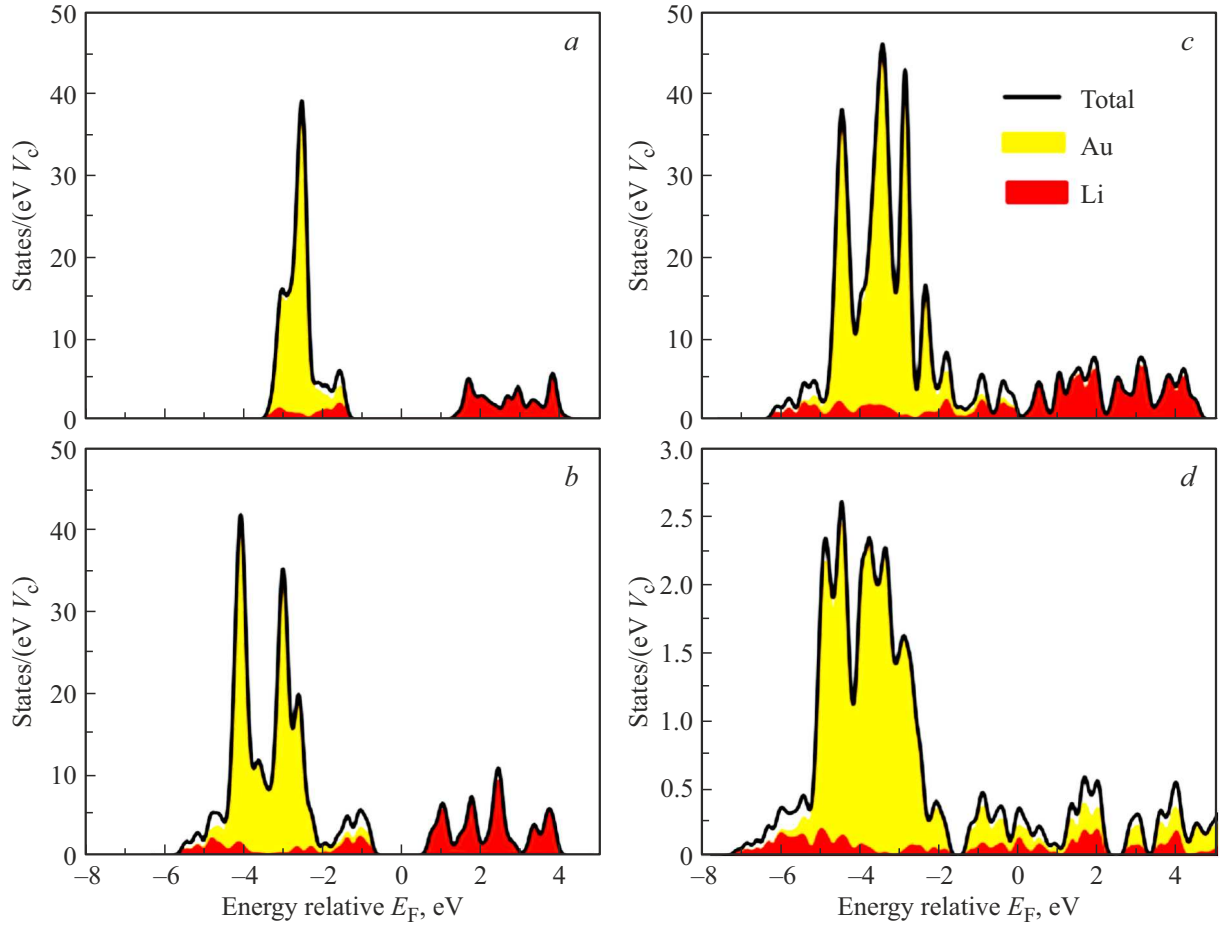

Figure 9. The calculated partial density of states for one LiAu layer (a) , two LiAu layers (b), three LiAu layers (c), total amount and density of states for LiAu (d). The Fermi level is set to 0 eV. Density of Au states is shown in yellow, Li — in red, and total DOS — in black.

from the calculation that LiAu is a metal and the calculation results are the same as the earlier calculations, e.g. [5,23]. There is a narrow band at the Fermi level which is indicative of the metallic nature of LiAu and is composed of 5d-, 6s- and 6p-states of Au and admixture of 2p-states of Li. The wide valence band has two poorly expressed maxima near -4.0 eV. The valence band is mainly formed by electrons of 5d-states of Au with a small admixture of 2p-states of Li. Contribution of Li electrons to the valence band is negligible and is indicative of the charge transfer from Li atoms to gold atoms. The vacant state band is mainly formed by Li 2s- and 2p-electrons with a negligible contribution of Au 6p- and 6s-electrons.

DOS calculation results for one LiAu monolayer are shown in Figure 9, a. The valence band bottom width is 2.55 eV, which is much lower than that of LiAu crystal. A wide band gap with $E_g = 2.0$ eV can be seen in the spectrum. The valence band maximum is by -1.41 eV lower than the Fermi level. The DOS maximum is at -2.51 eV and the band is mainly formed by Au 5d atom electrons. A small band with its maximum at -1.57 eV is mainly formed by 6s-electrons of Au with a negligible contribution of Li 2s- and 2p-electrons. The conduction band is mainly formed by Li 2s- and 2p-electrons with a negligible contribution of Au 6p-electrons.

DOS calculation results for two LiAu monolayers in thickness are shown in Figure 9, b. The valence band bottom width increases up to 5.1 eV LiAu. The band gap decreases to $E_g = 1.05$ eV. Two main maxima are observed in the valence band spectrum at -2.93 and -4.08 eV below the Fermi level and the band is mainly formed by Au 5d atom electrons. A small band with its maximum at -1.10 eV is mainly formed by 6s-electrons of Au with a negligible contribution of Li 2s- and 2p-electrons. The conduction band is mainly formed by Li 2s- and 2p-electrons with a negligible contribution of Au 6p-electrons. Occurrence of the additional peak is associated with the fact that the surface layer on different sides of the 2D layer was formed by different (Li or Au) atoms and a central layer occurs (see Figure 2, c). Calculated full and partial density of states for one 2D LiAu layer with thickness equal to two monolayers is shown in Figure 10.

DOS calculation results for three LiAu monolayers in thickness are shown in Figure 9, c. The band gap disappears.

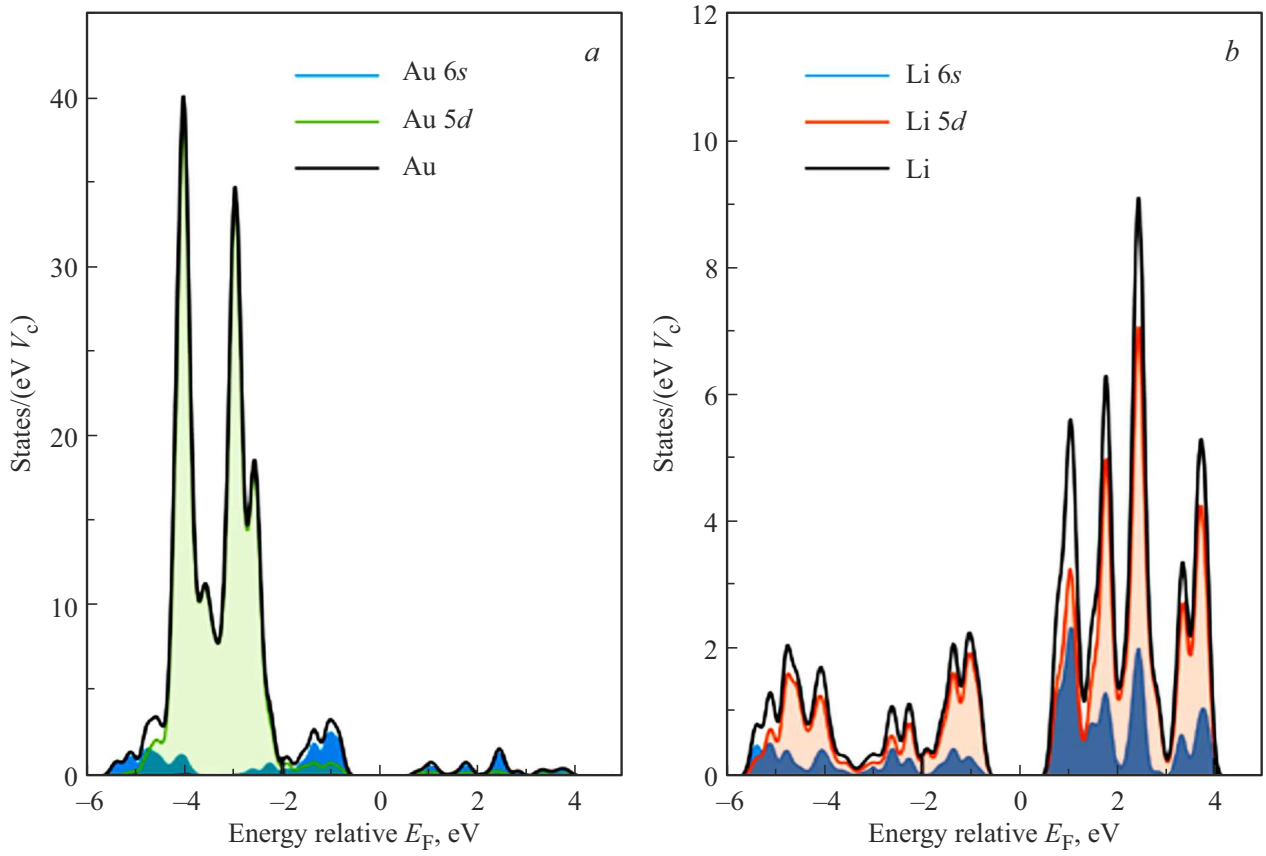

Figure 10. Calculated full and partial density of states for one 2D LiAu layer with thickness equal to two monolayers (*a, b*). The Fermi level corresponds to 0 eV. *a* Au 6*s*-states are shown in red, Au 5*d* states are shown in blue. Full density of Au states is shown in black. *b* Full density of Li states is shown in black, Li 2*s*-states are shown in blue, Li 2*p* states are shown in red.

The valence band bottom width increases up to 6.5 eV. The valence band maxima are at −3.0, −3.46 and −4.55 eV below the Fermi level and the band is mainly formed by Au 5*d* atom electrons. Several small bands occur below the Fermi level which are mainly formed by 6*s*-electrons of Au with a negligible contribution of Li 2*s*- and 2*p*-electrons. The conduction band is mainly formed by Li 2*s* and 2*p* electrons with a negligible contribution of Au 6*p*-electrons. The valence band view approaches that of LiAu crystal.

The calculations of density of states of 2D LiAu layers show that such 2D layers may be semiconductors. This result correlates with the observation of Li atom ESD from the LiAu intermetallic surface obtained by deposition of Li atoms on the thin gold film. ESD of atoms is recorded only from the semiconductor or dielectric surface with excitation energy lower than 200 eV. With an increase in 2D LiAu intermetallic thickness, the band gap decreases, which is indicative of the semiconductor-metal transition.

Our calculations of isolated 2D LiAu intermetallic layers cannot explain all observed effects during the Li atom ESD from the Li_xAu_y surface. The calculation only supports the semiconductor nature of the 2D Li_xAu_y intermetallics.

4. Conclusion

The study investigates the temperature effect on the Li atom ESD yield from the surface of 2D lithium-gold intermetallic semiconductor layer in the temperature range from 160 to 300 K. It is shown that the Li atom ESD yield is lower with lower temperature. This is associated with the features of processes occurring during the Li atom ESD: the highest influence is exerted by the fact that the probability of electron capture in the conduction band from the excited state near the conduction band bottom decreases with lower temperature. The Li atom ESD excitation process is associated with excitation of Au $5p_{3/2}$ and Au $5p_{1/2}$ core levels. Generally, excitation of Li 1*s* core levels is also possible and probably causes the peak asymmetry with its maximum at excitation energy 64 eV. The low-energy peak is associated with the Li atom ESD from the 2D lithium-gold intermetallic layer and the high-energy peak is associated with the Li atom ESD from the surface Li atom monolayer. An island model of 2D lithium-gold intermetallic layer formation during lithium atom deposition on the 2D gold layer is proposed. Density of electronic states of 2D LiAu intermetallic layers was calculated. It is shown that 2D LiAu layers consisting of a film 1−2 monolayers in thickness

are semiconductors, while thicker films are metallic. The valence band of 2D LiAu intermetallic layers is mainly formed by electrons of Au 5*d*-states with a small admixture of Au 5*s*-states with a negligible contribution of electrons of Li 2*p*-states.

Conflict of interest

The authors declare that they have no conflict of interest.

References

[1] M. Jansen. Chem. Soc. Rev. **37**, *9*, 1826 (2008).
[2] W.E. Spicer. Nature **152**, *3851*, 215 (1943).
[3] W.E. Spicer, A.N. Sommer, J.G. White. Phys. Rev. **115**, *1*, 57 (1959).
[4] H. Overhof, J. Knecht, R. Fischer. J. Phys. F **8**, *7*, 1607 (1978).
[5] R.E. Watson, M. Weinert. Phys. Rev. B **49**, *11*, 7148 (1994).
[6] G.H. Grosch, K.-J. Range. J. Alloys Comp. **233**, *1–2*, 30 (1996).
[7] J.A. Rodriguez, J. Hrbek, Y.-W. Yang, M. Kuhn, T.K. Sham. Surf. Sci. **293**, *3*, 260 (1993).
[8] Yu.A. Kuznetsov, M.N. Lapushkin. FTT **63**, *10*, 1701 (2021). (in Russian).
[9] M.V. Knat'ko, M.L. Lapushkin, V.I. Paleev. Phys. Low-Dime. Struct. **9–10**, 85 (1999).
[10] M.V. Knat'ko, M.N. Lapushkin, V.I. Paleev. ZhTF **68**, *10*, 108 (1998). (in Russian).
[11] V.N. Ageev, Yu.A. Kuznetsov. FTT **50**, *2*, 365 (2008). (in Russian).
[12] Yu.A. Kuznetsov, M.N. Lapushkin. FTT **62**, *11*, 1949 (2020). (in Russian).
[13] Yu.A. Kuznetsov, M.N. Lapushkin, N.D. Potekhina. Pis'ma v ZhTF **42**, *12*, 14 (2016). (in Russian).
[14] V.N. Ageev. Prog. Surf. Sci. **47**, 55 (1994).
[15] T.E. Madey. Surf. Sci. **299/300**, 824 (1994).
[16] V.N. Ageev, E.Yu. Afanaseva. FTT **48**, *8*, 2217 (2006). (in Russian).
[17] U.Kh. Rasulev, E.Ya. Zandberg. Prog. Surf. Sci. **28**, *3–4*, 181 (1988).
[18] P. Giannozzi, S. Baroni, N. Bonini, M. Calandra, R. Car, C. Cavazzoni, D. Ceresoli, G.L. Chiarotti, M. Cococcioni, I. Dabo, A.D. Corso, S. de Gironcoli, S. Fabris, G. Fratesi, R. Gebauer, U. Gerstmann, C. Gougoussis, A. Kokalj, M. Lazzeri, L. Martin-Samos, N. Marzari, F. Mauri, R. Mazzarello, S. Paolini, A. Pasquarello, L. Paulatto, C. Sbraccia, S. Scandolo, G. Sclauzero, A.P. Seitsonen, A. Smogunov, P. Umari, R.M. Wentzcovitch. J. Phys. Condens. Mater. **21**, *39*, 395502 (2009).
[19] J.P. Perdew, K. Burke, M. Ernzerhof. Phys. Rev. Lett. **77**, *18*, 3865 (1996).
[20] J.P. Perdew, J.A. Chevary, S.H. Vosko, K.A. Jackson, M.R. Pederson, D.J. Singh, C. Fiolhais. Phys. Rev. B **46**, *11*, 6671 (1992).
[21] N. Troullier, J.L. Martins. Phys. Rev. B **43**, *3*, 1993 (1991).
[22] S. Nishihara. BURAI 1.3 A GUI of Quantum ESPRESSO. https://nisihara.wixsite.com/burai (accessed 04 April 2023).
[23] C. Koenig, N.E. Christensen. J. Collar. Phys. Rev. B **29**, *12*, 6481 (1984).

Translated by Ego Translating